



APPLICATION OF SUBSPACE-BASED BLIND IDENTIFICATION METHOD IN STRUCTURAL SYSTEMS

Songtao Liao¹ and Aspasia Zerva²

SUMMARY

A subspace-based blind system identification algorithm developed in the communications area by Moulines *et al.* [1] is introduced into structural dynamics problems. The approach requires at least two recorded/measured data series at different locations of the same structure or at different structures subjected to the same seismic excitation. The technique does not require any prior information about the characteristics of the structure(s) and the input excitation. The subspace-based blind identification scheme constructs a Sylvester matrix from the second-order statistics of the output data, and applies eigenvalue decomposition to the matrix. The impulse response functions of the structure(s) can be identified from the signal subspace or the noise subspace. After the impulse response functions have been identified, the unknown input excitation can also be reconstructed through equalization. The performance of the subspace-based blind identification method in structural systems is illustrated with three examples of simulated data: it is shown that the technique can identify the structural impulse response functions and reconstruct the input excitation with high degree of accuracy in both time and frequency domains.

INTRODUCTION

System identification is widely used in structural control, health monitoring and geologic subsurface information extraction. In conventional system identification methods, both the input excitation and the output response are measured, and then the structural system characteristics are identified [2,3]. However, in cases, only the output signals are available because of the obstructive difficulty to set up special experiments or impossibility to record the input data. This type of output-only system identification problem is utilized, for example, in operational modal analyses, ambient vibrations surveys and blind identifications [4-6].

A number of output-only identification methods have been proposed in both frequency and time domains, such as the complex mode indication functions method [7], the instrumental variable methods [8] and the stochastic subspace identification methods [9], to name a few traditional ones. In addition to the traditional approaches for output-only system identification, some new techniques, geared more towards civil engineering problems, have appeared in the literature. For example, based on the statistical properties of a spectral estimator, Katafygiotis and Yuen [5] studied the output-only, parametric problem of

¹ Graduate Research Assistant, Drexel University, Philadelphia, USA. E-mail: Songtao.Liao@drexel.edu

² Professor, Drexel University, Philadelphia, USA. E-mail: Aspasia.Zerva@drexel.edu

structural modal parameter identification with the Bayesian spectral density approach. The methodology provides not only the optimal values of the modal parameters but also their uncertainties.

Parametric system identification techniques, however, by assuming a model for the system, provide only an approximation to the system. For example, modal damping used in the structural models is a necessary but artificial device. Blind (nonparametric) system identification techniques, on the other hand, do not require any physical or mathematical model for the system. Additionally, if more than one measured output recordings are available, then the techniques relax the assumption that the input excitation has to be white noise, as is the case for the commonly used frequency-domain, peak-picking method [10]. Zerva *et al.* [6] applied such a nonparametric, blind identification scheme based on reconstruction from phase methodology [11] in site response analysis. In this method, two recordings on the free surface of a sediment site are considered to be the result of the convolution of the incident earthquake motion at the bedrock-surface layer interface with the transfer functions of the seismic waves from the interface to the free surface. With this technique, the transfer functions are identified in both the time and frequency domains, and the input excitation is reconstructed through deconvolution of the output data with the identified impulse response functions.

The concept of nonparametric, blind system identification using second order statistics was introduced approximately ten years ago. Tong *et al.* [12] examined the cyclostationarity of an oversampled communication signal to equalize nonminimum phase channels. This blind identification scheme can guarantee that the estimates are asymptotically exact. Based on the idea of Tong *et al.* [12], a number of blind identification methods have been proposed, among which the subspace-based blind identification technique of Moulines *et al.* [1] is a representative one. This subspace-based method identifies the signal transmission channel up to a scale factor in the time and frequency domains, and the corresponding input excitation can be reconstructed from the identified transfer functions. The subspace-based method is presently being extended by researchers in the field of communication [13].

This paper introduces the subspace-based blind identification method proposed by Moulines *et al.* [1] in structural dynamic systems to examine its applicability to these problems. The approach requires at least two recordings at different locations in a structure subjected to a seismic excitation, or at least two recordings in close-by structures subjected to the same seismic excitation. The impulse response functions of the structures are considered as the signal transmission channels. No parametric models for the impulse response functions are required and the input excitation is considered to be unknown. The methodology identifies the impulse response functions in the time and frequency domains and, through equalization, the time history of the input excitation. The performance of the subspace-based blind identification method in structural systems is illustrated with three examples.

SUBSPACE-BASED BLIND SYSTEM IDENTIFICATION METHODOLOGY

In the following, the approach by Moulines *et al.* [1] is presented in some detail: It is considered that an unknown input excitation is passing through (linear) unknown filters (termed “channels”). The output is then the result of the convolution of the input excitation with the characteristics of the filters. In structural dynamics, the input excitation would be, e.g., the seismic excitation at the base of the structure, and the “channels” would reflect the structural characteristics (impulse response functions) from the base to any degree-of-freedom in the structure. The recorded outputs at the various locations in the structure are considered to be known, and are the information used by the methodology to identify the impulse response functions of the structure from the base to the degrees-of-freedoms considered, and, through equalization, reconstruct the input seismic excitation. Parenthetically, it is noted that the output data can be recorded either at different degrees-of-freedom of a single structure or in several close-by structures subjected to the same excitation.

Based on the above considerations, the recorded system output signals can be modeled as follows:

$$x^{(i)}(t) = \sum_{m=0}^M d_m h^{(i)}(t - mT) + b^{(i)}(t) \quad (1)$$

in which, $x^{(i)}(t)$ denotes the i -th recorded (discrete) time series, d_m is the input excitation, $h^{(i)}(t)$ is the impulse response for the i -th channel, and $b^{(i)}(t)$ represents random noise corresponding to i -th channel. The output time series in Eq. (1), $x^{(i)}(t)$, are known, but no information is required for the input excitation, d_m , or the impulse response functions of the channels, $h^{(i)}(t)$. The blind identification scheme, described below, will identify the impulse response functions in both time and frequency domains [1].

Assume there are L channels in the problem considered, and the impulse response coefficients of each channel can be expressed as:

$$\mathbf{H}^{(i)} = [h_0^{(i)}, h_1^{(i)}, \dots, h_M^{(i)}]^T, \quad i = 1, \dots, L \quad (2)$$

in which $M+1$ is the number of the channel's filter coefficients. By stacking N successive samples of the recorded sequences for one channel, the following equation is obtained in matrix form:

$$\mathbf{X}_n^{(i)} = \mathbf{H}_N^{(i)} \mathbf{D}_n + \mathbf{B}_n^{(i)} \quad (3)$$

where: $\mathbf{X}_n^{(i)} = [x_n^{(i)}, x_{n-1}^{(i)}, \dots, x_{n-N+2}^{(i)}, x_{n-N+1}^{(i)}]^T$; $\mathbf{D}_n = [d_n, d_{n-1}, \dots, d_{n-N+1}]^T$;

$$\mathbf{B}_n^{(i)} = [b_n^{(i)}, b_{n-1}^{(i)}, \dots, b_{n-N+1}^{(i)}]^T; \quad \text{and}$$

$$\mathbf{H}_N^{(i)} = \begin{bmatrix} h_0^{(i)} & \dots & h_M^{(i)} & 0 & \dots & \dots & 0 \\ 0 & h_0^{(i)} & \dots & h_M^{(i)} & 0 & \dots & 0 \\ \vdots & \vdots & \vdots & \vdots & \vdots & \vdots & \vdots \\ 0 & \dots & \dots & 0 & h_0^{(i)} & \dots & h_M^{(i)} \end{bmatrix}, \quad (\text{dim. } N \times (M + N))$$

The filtering matrix $\mathbf{H}_N^{(i)}$ corresponds to the i th channel, and the $M+1$ unknown impulse coefficients are to be identified. In a similar way, the equations for the remaining $L-1$ channels can be obtained. By combining the relationships for all L channels, the following equation results:

$$\mathbf{X}_n = \mathbf{H}_N \mathbf{D}_n + \mathbf{B}_n \quad (4)$$

where \mathbf{H}_N is a Sylvester matrix. In order to identify the coefficients for all channels, the signal subspace and the noise subspace of the $LN \times LN$ autocorrelation matrix of \mathbf{X}_n are utilized. The corresponding autocorrelation matrix can be readily expressed as:

$$\mathbf{R}_X = E(\mathbf{X}_n \mathbf{X}_n^H) = \mathbf{H}_N \mathbf{R}_D \mathbf{H}_N^H + \mathbf{R}_B = \mathbf{H}_N \mathbf{R}_D \mathbf{H}_N^H + \sigma^2 \mathbf{I}_{LN \times LN} \quad (5)$$

Because \mathbf{R}_X is a Hermitian matrix ($\mathbf{R}_X = \mathbf{R}_X^*$), eigenvalue decomposition can be applied as:

$$\begin{aligned} \mathbf{R}_X &= [\mathbf{S} \quad \mathbf{G}] \begin{bmatrix} \sum_S & \mathbf{0} \\ \mathbf{0} & \sum_G \end{bmatrix} \begin{Bmatrix} \mathbf{S}^H \\ \mathbf{G}^H \end{Bmatrix} \\ &= \mathbf{S} \text{diag}(\lambda_0, \dots, \lambda_{M+N-1}) \mathbf{S}^H + \sigma^2 \mathbf{G} \mathbf{G}^H \end{aligned} \quad (6)$$

in which, \sum_S is the diagonal matrix of eigenvalues, $\lambda_i > \sigma^2$ for $i = 0, \dots, M + N - 1$, corresponding to the signal subspace eigenvectors \mathbf{S} , and \sum_G is the diagonal matrix of eigenvalues, $\lambda_i = \sigma^2$ for $i = M + N, \dots, LN - 1$, corresponding to the noise subspace eigenvectors \mathbf{G} . The eigenvectors $[\mathbf{S} \quad \mathbf{G}]$ constitute an orthonormal set. The signal subspace is the linear space spanned by the columns of

the filtering matrix \mathbf{H}_N in Eq. (4). With this property and the orthogonality property between the signal and noise subspaces, the following relationship holds:

$$\mathbf{G}_i^H \mathbf{H}_N = \mathbf{0}, \quad 0 \leq i < LN - M - N \quad (8)$$

In practice only sample estimates $\hat{\mathbf{G}}_i$ are available, and Eq. (8) can be solved in the least-squares sense, using the sample estimate, $\hat{\mathbf{G}}_i$, rather than its actual value, \mathbf{G}_i , i.e., through the minimization of the following equation:

$$q(\mathbf{H}) = \sum_{i=0}^{LN-M-N-1} \left| \hat{\mathbf{G}}_i^H \mathbf{H}_N \right|^2 \quad (9)$$

It needs to be emphasized that the number of channels, i.e., recordings, should be $L \geq 2$, and that the number of recorded time steps (N) should be greater than the duration ($M+1$) of the impulse response functions (channels) minus one, i.e., $N \geq M$, otherwise Eqs. (8) become underdetermined, and the identification fails. The squared norm of the vector in Eq. (9), becomes then:

$$\left| \hat{\mathbf{G}}_i^H \mathbf{H}_N \right|^2 = \hat{\mathbf{G}}_i^H \mathbf{H}_N \mathbf{H}_N^H \hat{\mathbf{G}}_i = \mathbf{H}^H \hat{\mathbf{Q}}_i \hat{\mathbf{Q}}_i^H \mathbf{H} \quad (10)$$

or, alternatively,

$$q(\mathbf{H}) = \mathbf{H}^H \mathbf{Q} \mathbf{H} \quad \text{where} \quad \mathbf{Q} = \sum_{i=0}^{LN-M-N-1} \hat{\mathbf{Q}}_i \hat{\mathbf{Q}}_i^H \quad (11)$$

The problem then reduces to the minimization of $q(\mathbf{H})$ as expressed by Eq. (11). Under the condition $|\mathbf{H}|=1$, the solution is the unit-norm eigenvector associated to the smallest eigenvalue of the matrix \mathbf{Q} . Alternatively, the signal subspace can be utilized [1], and the analyses using the signal and the noise subspace provide identical solutions. It should be noted that the channel coefficients, $\mathbf{H}_N^{(i)}$, can be identified up to a multiplication constant, which is inherent to this type of methodologies, as well as a time shift in the time domain identification, as there is no absolute time defined in the inverse problem. For structural systems, the channel filter coefficients correspond to the impulse response functions of the structure, from which the input excitation can be reconstructed.

Once the channel coefficients have been identified either from the signal or the noise subspace, the input excitation can be reconstructed through equalization from the following expression [1]:

$$\mathbf{E} = \mathbf{H}_N^H \mathbf{S} \text{diag}(\lambda_0, \dots, \lambda_{M+N-1}) \mathbf{S}^H \quad (12)$$

with parameters as specified in Eq. (6).

NUMERICAL EXAMPLES AND DISCUSSION

Three examples are presented herein to investigate the potential applicability of the subspace-based blind identification algorithm [1] in structural dynamic analysis. All examples deal with simulated data: an idealized model of a structure (or structures) is constructed and its impulse response functions at a number of degrees-of-freedom are determined analytically/numerically. A seismic excitation or a random process is considered then to excite the system(s). Convolution is used to transfer the input excitation from the base of the structure(s) to the degrees of freedom specified. The outcome of this process is considered to be the “recorded output time series” at the structure’s locations. Only these “recorded output time series” are considered in the blind system identification. The analytically evaluated impulse response functions and the actual input excitation are used only for comparison with the blindly identified system and input characteristics.

Example 1:

The first example is a lumped-mass system with two degrees-of-freedom, as indicated in Fig. 1. The dynamic equation of motion for the system (dimensionless values) is given by:

$$\begin{bmatrix} 6 & -2 \\ -2 & 6 \end{bmatrix} \begin{Bmatrix} \ddot{u}_1 \\ \ddot{u}_2 \end{Bmatrix} + \begin{bmatrix} 1.2 & -0.4 \\ -0.4 & 1.2 \end{bmatrix} \begin{Bmatrix} \dot{u}_1 \\ \dot{u}_2 \end{Bmatrix} + \begin{bmatrix} 2 & 0 \\ 0 & 1 \end{bmatrix} \begin{Bmatrix} u_1 \\ u_2 \end{Bmatrix} = \{f\} \quad (13)$$

in which u_1, u_2 are the displacements at degree-of-freedom (d.o.f.) 1 and d.o.f. 2, respectively, and \dot{u}_i, \ddot{u}_i , $i = 1, 2$, indicate velocity and acceleration. The actual impulse response functions of the model can be readily obtained from Eq. (13). This idealized structure is then subjected to the seismic excitation presented in Fig. 2. In this example, the time and frequency domain units are normalized, so that some terms used in the previous section can be clarified. The convolution of the excitation in Fig. 2 with the structure's (Fig. 1) impulse response functions (also provided in time steps) result in the "recorded output data" presented in Fig. 3; the order (or, essentially, the duration) of the impulse response functions was considered to be 40 time steps. The time histories of Fig. 3 are the only information used in the subspace-based blind identification algorithm.

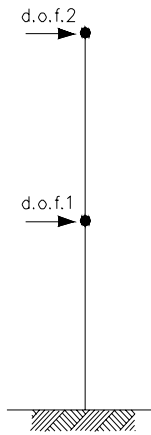


Figure 1 Lumped-mass model with two degrees-of-freedom

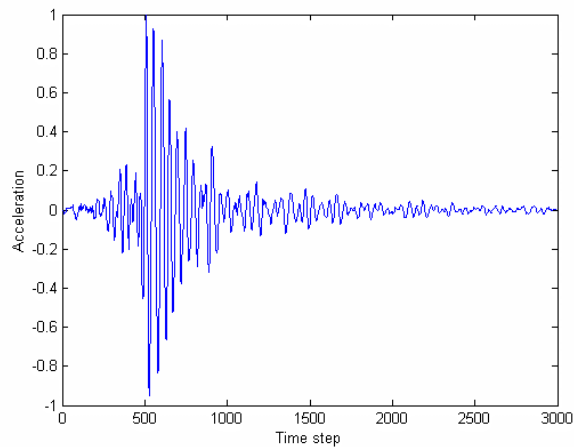


Figure 2 Sample acceleration time history used as input excitation

Figure 4 compares the actual impulse response functions (solid, blue lines) with the identified ones (dash, red lines) in both time and frequency domains. Because the system identification scheme determines the system's characteristics within a multiplication factor, all comparisons presented in Fig. 4 and hereafter are made with normalized quantities. The time domain comparison in Fig. 4 indicates also the effect of the time shift that is commonly present in this type of identifications. The results (actual and identified) in Fig. 4 are in excellent agreement. For the impulse response function at d.o.f. 1, the algorithm identifies a dominant peak, and for that of d.o.f. 2, two dominant peaks at close-by frequencies. The results at both degrees-of-freedom suggest a small peak past the dominant ones, and their frequency content tends to zero quicker than that of the actual response functions. Based on the identified impulse response functions and the output recordings, the "unknown" input excitation can be reconstructed. The comparison of the reconstructed with the actual input excitation in time and frequency domains is shown in Fig. 5; again, for comparison purposes the results are normalized. The normalized curves agree well with each other in both time and frequency domains.

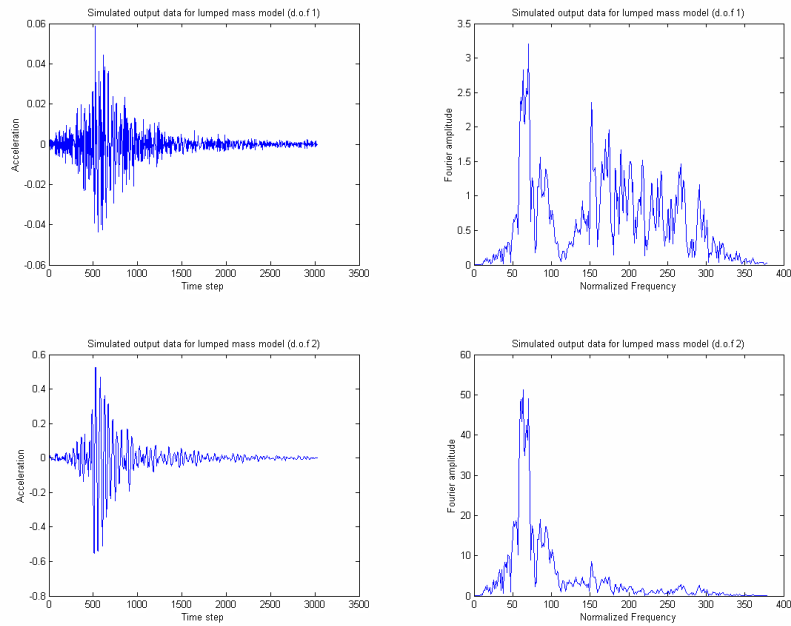


Figure 3 Time and frequency domain characteristics of the response at degrees-of-freedom 1 and 2 of the system presented in Fig. 1 subjected to the excitation of Fig.2

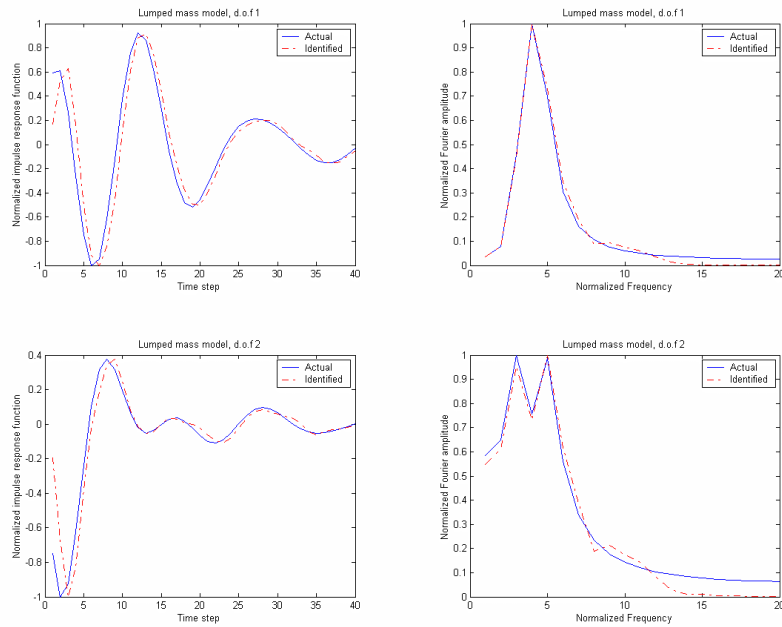


Figure 4 Comparison of normalized impulse response functions in time and frequency domains at degrees-of-freedom 1 and 2 of the lumped-mass model shown in Fig. 1

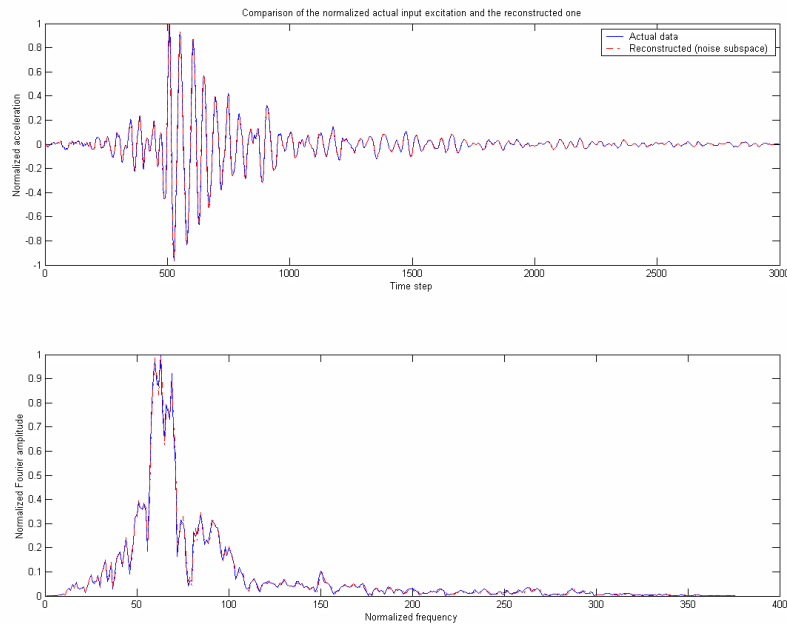


Figure 5 Comparison of the identified input excitation with the actual one

Example 2:

The second example deals with an idealized structure (Fig. 6) subjected to the ground motions recorded in the east-west direction at station No. 1 of the Leona Valley array during the Northridge earthquake (Fig. 7). The idealized structure is actually a shear wall, 12 m high and 2 m wide. The structural properties are assumed to be: density $\rho = 1800 \text{ kg/m}^3$, elasticity coefficient $E = 9.0 \times 10^7 \text{ Pa}$, Poisson ratio $\nu = 0.3$. Rayleigh damping is utilized with $\alpha = 4.693$ and $\beta = 3.350$. The impulse response functions of the systems from the base to the horizontal and vertical d.o.f. at the upper left corner (Fig. 6) are evaluated by means of the finite element method using a $1.0 \text{ m} \times 1.0 \text{ m}$ grid; the order of the impulse response functions used hereafter is 28. The time step is $\Delta t = 0.02 \text{ sec}$.

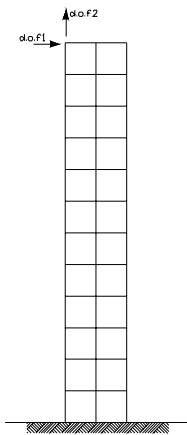


Figure 6 Shear wall structure used in Example 2

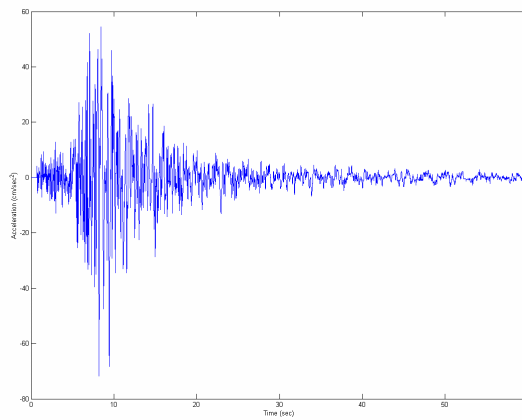


Figure 7 Northridge earthquake recorded at station No.1 of the Leona Valley array

The impulse response functions of the structure, evaluated numerically, are then convolved with the seismic excitation. The results of the convolution in time and frequency domains are presented in Fig. 8. Figure 8 is, again, the only information used by the algorithm to identify the system's impulse response functions and the seismic excitation.

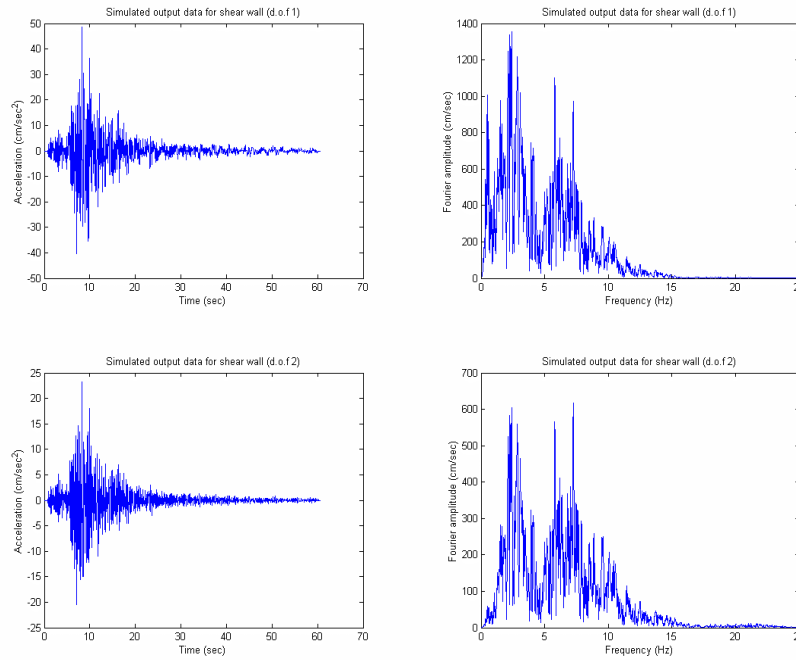


Figure 8 Time and frequency domain characteristics of the response at degrees-of-freedom 1 and 2 of the shear wall of Fig. 6 subjected to the excitation of Fig. 7

Figure 9 presents the comparison of the identified with the actual normalized response functions of the system for the degrees-of-freedom considered. As has been indicated before, since the approach identifies the system's characteristics within a multiplication constant, the amplitudes of both time and frequency domain data have been normalized. The agreement is essentially perfect. It is noted that, in this case, no time shift is obvious from the figures. Figure 10 then presents the comparison of the actual and reconstructed normalized input excitation in the time and frequency domains. As expected from the agreement of the results in Fig. 9, the reconstructed input excitation is basically identical to the actual one.

The perfect match between the identified and actual characteristics of the system and the input excitation in this example does not guarantee that the algorithm will always produce such accurate results. For example, the same structure was subjected to a different seismic excitation and the results "recorded" at the same two degrees of freedom shown in Fig. 6. Although the comparison was very good (results not shown herein), it was not perfect as that of Figs. 9 and 10. It appears then that identifiability criteria need to be established for this as well as other blind system identification algorithms using simulated data, such the ones presented herein, before these algorithms can be readily used with seismic data recorded in real structures. The establishment of such criteria is presently underway.

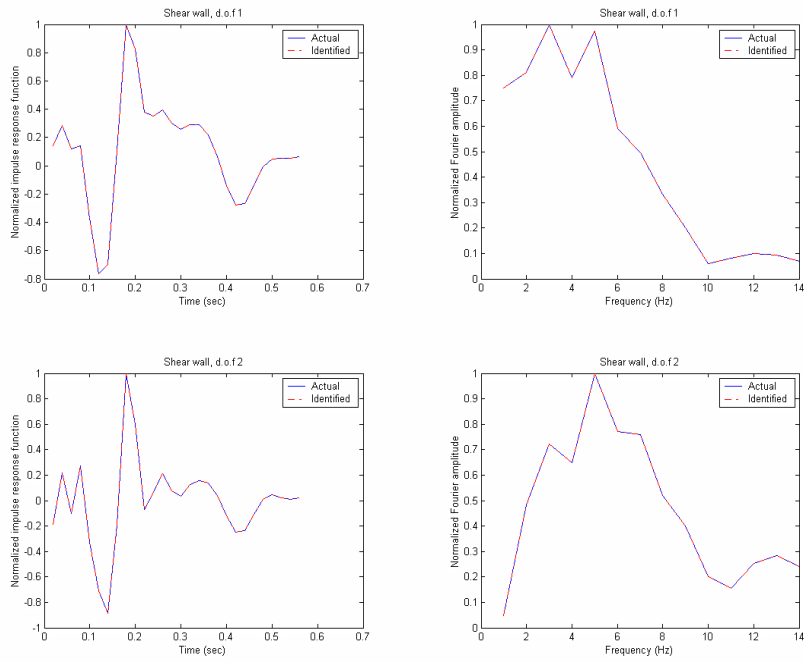


Figure 9 Comparison of normalized impulse response functions in time and frequency domains at degrees-of-freedom 1 and 2 of the shear wall model shown in Fig. 6

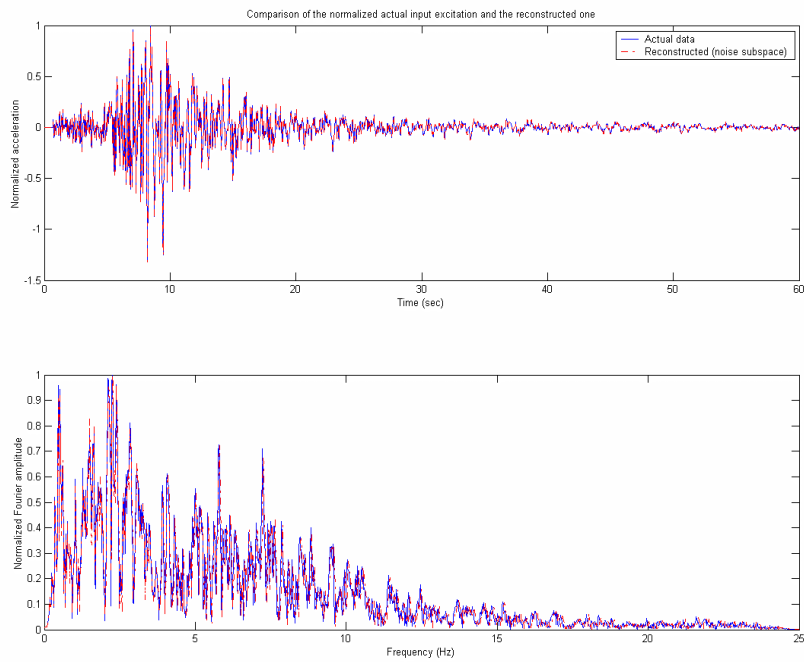


Figure 10 Comparison of the identified input excitation with the actual one

Example 3:

This last example considers two different idealized structures subjected to the same seismic excitation. Figure 11 presents two shear walls of different heights: one is 12 m (the same one as in Fig. 6) and the other 8 m high; the width of both models is 2 m. The same mechanical properties as those of the shear wall in Example 2 are utilized. The impulse response function of these systems from the base to their respective top left corner (Fig. 11) are evaluated by means of the finite element method; the order of the impulse response functions is, again, 28. In this example, the input excitation is generated as a normally distributed random number time series (Fig. 12); the time step is $\Delta t = 0.02$ sec. The impulse response functions of the structures are then convolved with the input (noise) excitation. Additionally, white Gaussian noise is added to the simulated output data with a signal-to-noise ratio (SNR) of 45dB, so as to reflect additive noise at the recording location. Here SNR is defined as: $SNR = 10 \log_{10}(\sigma_s^2 / \sigma_n^2)$, where σ_s^2 and σ_n^2 are the variance of the signal and noise, respectively. The results of these operations are presented in Fig. 13 in the time and frequency domains. The output data presented in Fig. 13 are, again, the only information used in the identification process.

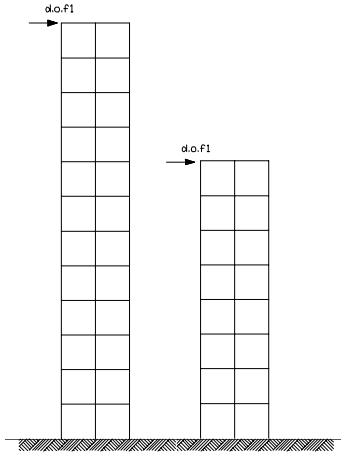


Figure 11 Two idealized models (shear walls) of different height

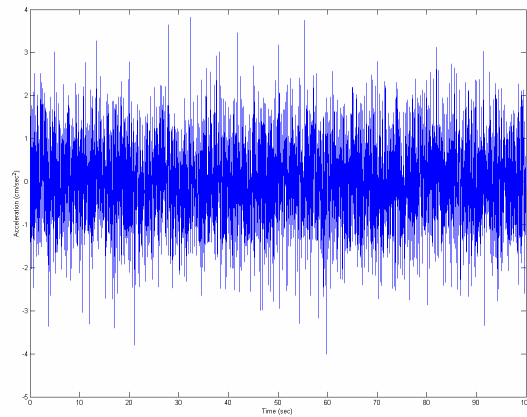


Figure 12 Normally distributed random number time series used as input excitation in example 3

Figure 14 presents the results of the system identification. The subspace-based blind scheme again identifies with very good accuracy the impulse response functions of the systems in both time and frequency domains. As in the first example presented herein, there is a slight time shift in the time domain results, a fact that is inherent in this type of algorithms. In this case, however, there appears to be a slight additional “delay” in the location of the peaks of the impulse response functions. Furthermore, the identified impulse response functions slightly underestimate the actual ones in the higher frequency range. The reconstructed input motion obtained through equalization of the output data with the identified impulse response functions is presented in Fig. 15. The reconstructed normalized input excitation does not fully agree with the actual one, as was the case in the first two examples, although its trends in the time and frequency domain are captured. However, some irregular peaks of the actual input excitation are lost in the reconstructed input data. These discrepancies between the actual and reconstructed characteristics in this example are strongly related to the presence of the additive noise at the “recording” locations. A SNR ratio for the additive noise lower than the one used herein would not produce the satisfactory results of Figs. 14 and 15 (results not shown herein). The effect of noise in this type of system identification is also an important consideration that requires additional evaluation; efforts in this direction are also currently under way.

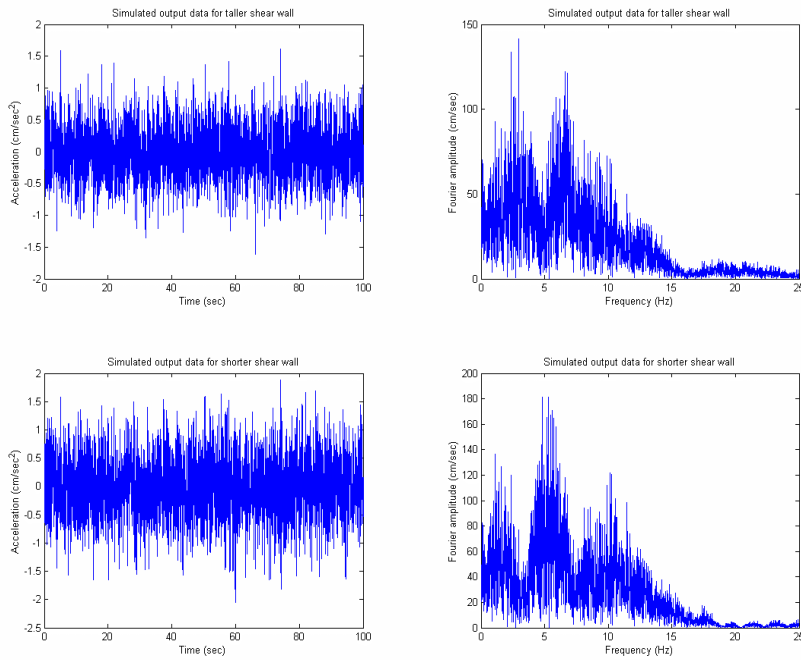


Figure 13 Time and frequency domain characteristics of the response of the taller and the shorter shear wall structures of Fig. 11 subjected to the noise excitation of Fig. 12

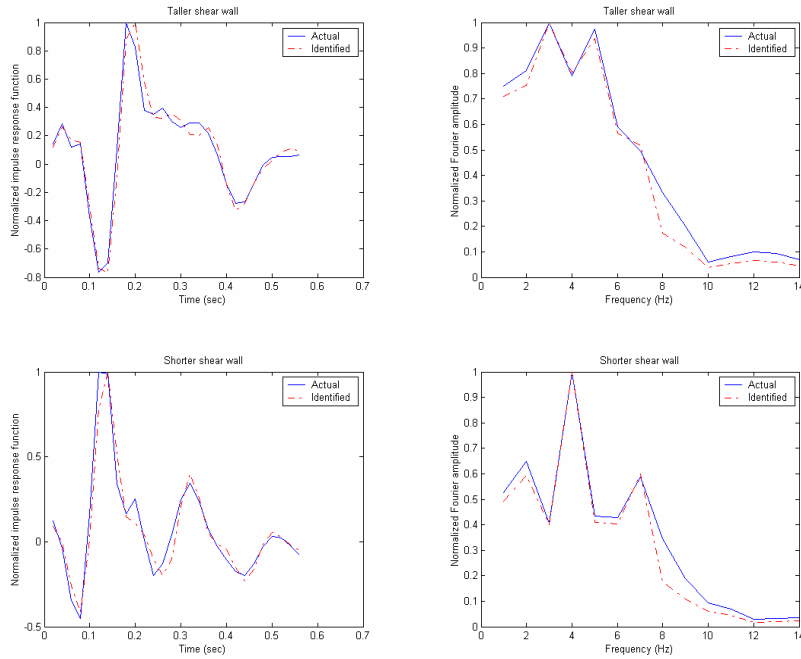


Figure 14 Comparison of normalized impulse response functions in time and frequency domains of the two shear wall models shown in Fig.11

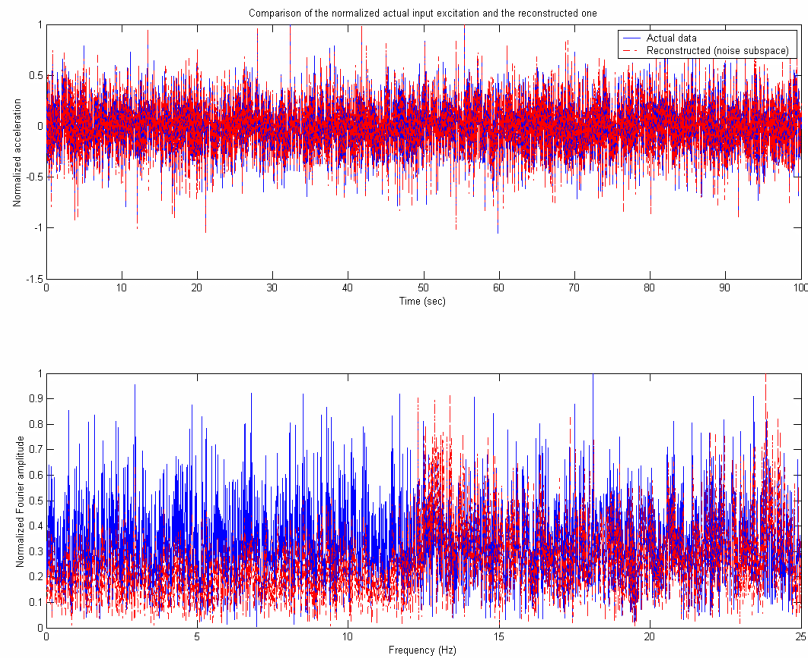


Figure 15 Comparison of the identified input excitation with the actual one

CONCLUSIONS

The subspace-based blind system identification technique developed by Moulines *et al.* [1] was introduced into structural dynamics problems in this paper. The algorithm requires at least two recorded data series at two different locations (or degrees-of-freedom) of the same structure or at different structures subjected to the same seismic excitation. The method does not require any prior information about the characteristics of the structure(s) and the input excitation, and, also, does not require that the input excitation is white noise. The subspace-based blind identification scheme used herein constructs a Sylvester matrix from the second-order statistics of the output data, and applies eigenvalue decomposition to the matrix. The impulse response functions of the structure(s) can be identified from the signal subspace or the noise subspace. Inherent in this type of blind system identification is the fact that the results are identified within a multiplication constant and a time shift. After the impulse response functions have been identified, the unknown input excitation can also be reconstructed.

The potential applicability of the blind identification method in structural systems is illustrated herein with three examples. In all cases, the “recorded output” data were simulated using as input motions actual seismic recordings or noise and as impulse response functions those of idealized structural models. The information, however, on the excitation and the structural systems was not used in the identification, but only in the comparison of the identified characteristics with the actual ones. All three examples indicated that the technique can identify the structural and input motion characteristics to a very satisfactory degree. However, system identification is, in many cases, an ill-conditioned and non-unique inverse problem, and blind system identification algorithms have the same disadvantages. Issues of identifiability in these techniques are important concerns. Research in this direction is currently underway.

REFERENCES

1. Moulines E., Duhamel P., Cardoso J.F., Mayrargue S., "Subspace methods for the blind identification of multichannel FIR filters", IEEE, Transaction on Signal Processing, 1995; 43(2): 516-525.
2. Ghanem R., Shinozuka M., "Structural-system identification I: theory", Journal of Engineering Mechanics, ASCE, 1995; 121(2): 255-264.
3. Ljung L., System identification: theory for the user, 2nd edition, Prentice Hall Inc. 1999.
4. Peeters B., De Roeck G., "Stochastic system identification for operational modal analysis: a review", Journal of Dynamic Systems, Measurement, and Control, 2001; 123: 659-667.
5. Katafygiotis L.S., Yuen K.V., "Bayesian spectral density approach for modal updating using ambient data", Earthquake Engineering and Structural Dynamics, 2001; 30: 1103-1123.
6. Zerva A., Petropulu A.P., Bard P.Y., "Blind deconvolution methodology for site-response evaluation exclusively from ground-surface seismic recordings", Soil Dynamics and Earthquake Engineering, 1999; 18: 47-57.
7. Shih C.Y., Tsuei Y.G., Allemang R.J., Brown D.L., "Complex mode identification function and its application to spatial domain parameter estimation", Mech. Syst. Signal Process, 1988; 2(4): 367-377.
8. Young P.C., "An instrumental variable method for real-time identification of a noisy process", Automatica, 1970; 6: 271-287.
9. Van Overschee P., De Moor B., "Subspace identification for linear systems: theory-implementation-application", Kluwer Academic Publishers, 1996.
10. Bendat J.S., Piersol, A.G. Engineering applications of correlation and spectral analysis, John Wiley and Sons, Inc., 1993.
11. Pozidis, H., Petropulu, A.P., "Cross-spectrum based blind channel identification", IEEE Transactions on Signal Processing, 1997; 45: 2997-2993.
12. Tong L., Xu G., Kailath T., "Blind identification and equalization based on second-order statistics: a time domain approach", IEEE Transactions on Information Theory, 1994; 40(2): 340-390.
13. Liavas A.P., Regalia P.A., Delmas J.P., "Blind channel approximation: effective channel order determination", IEEE, Transaction on Signal Processing, 1999; 47(12): 3336-3344.